

Structural and Magnetic Properties of Ultrathin Fe Films on Pt(001) Surface

This article has been downloaded from IOPscience. Please scroll down to see the full text article.

2005 Chinese Phys. Lett. 22 203

(<http://iopscience.iop.org/0256-307X/22/1/058>)

View [the table of contents for this issue](#), or go to the [journal homepage](#) for more

Download details:

IP Address: 159.226.35.179

The article was downloaded on 10/07/2011 at 07:53

Please note that [terms and conditions apply](#).

Structural and Magnetic Properties of Ultrathin Fe Films on Pt(001) Surface *

ZHANG Li-Juan(张丽娟), HE Ke(何珂)**, JIA Jin-Feng(贾金锋), XUE Qi-Kun(薛其坤)

State Key Laboratory for Surface Physics and International Centre for Quantum Structures, Institute of Physics, Chinese Academy of Sciences, Beijing 100080

(Received 20 August 2004)

Magnetic anisotropy evolution of ultrathin Fe films grown on Pt(001) single-crystal surface is investigated by UHV in situ surface magneto-optical Kerr effect (SMOKE) measurement. After annealing at ~ 600 K, the magnetic anisotropy of Fe film switches from in-plane to perpendicular at low coverage, leading to a spin reorientation transition (SRT). Meanwhile, in the range of 3–4 monolayer (ML) thickness, the coercivity of the Fe polar hysteresis loop decreases dramatically. Further scanning tunnelling microscopy (STM) and low energy electron diffraction (LEED) investigation correlates the magnetic properties with the film structures. We attribute this SRT to the formation of Fe–Pt ordered alloy.

PACS: 75.30.Gw, 75.70.Ak, 75.70.Rf

Magnetic anisotropy is one of the most technologically important properties of magnetic materials. In the past two decades, a great deal of attention has been paid to the growth of ultrathin ferromagnetic metal films on nonmagnetic substrates and the evolution of magnetic properties in such systems.^[1,2] The reduced dimensionality induces many extraordinary magnetic properties such as perpendicular magnetic anisotropy (PMA), enhanced magnetic moment, and spin reorientation transition (SRT).^[3] For the case of Fe/Pt(001) multilayers, the relationship between structure and magnetic anisotropy has been investigated by Sakurai,^[4] Visokay *et al.*,^[5] and Hufnagel *et al.*^[6] However, to our best knowledge, study of Fe ultrathin films on Pt(001) single crystal surface is relatively scarce. In this Letter, we present our results obtained using efficient surface analysis and magnetic measurement instruments on the Fe/Pt(001) system.

All our experiments were carried out in a multifunctional ultrahigh vacuum system equipped with scanning tunnelling microscope (STM), low energy electron diffraction (LEED), and surface magneto-optic Kerr effect (SMOKE) measurement. The base pressure of the system was kept below 8×10^{-11} mbar. The Pt(001) single crystal surface was cleaned by cycles of Ar⁺ sputtering at 1 keV and annealing at ~ 1000 K until sharp fivefold LEED spots were observed [Fig. 1(a)], meanwhile STM images [Fig. 1(b)] revealed well defined rowlike reconstruction.^[7–9] The Fe was evaporated from a resistively heated Ta boat and deposited on the substrate as either a stepped sample or a wedged sample to facilitate measurement efficiency and continued growth of Fe films throughout the experiment. The thickness of the Fe film was determined by STM calibration. The typical Fe evaporation rate was 1 ML/9 min.

Structural properties of the film were characterized by STM and LEED at room temperature. LEED measurements were performed along the Fe wedge for different Fe thicknesses. Uniform or stepped films were grown for STM studies. A dc-etched tungsten tip was used for imaging. All images reported here were obtained with a tunnelling current of 20 pA.

A home made *in situ* SMOKE setup can provide detailed information on the evolution of magnetic anisotropy such as SRT when measured in ultrahigh vacuum.

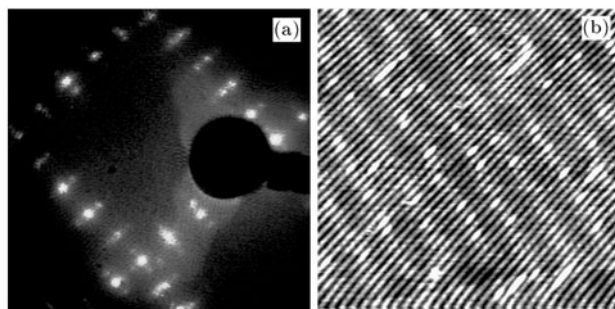


Fig. 1. STM image and LEED pattern of clean Pt(001)-hex surface. The STM image size is $50 \times 50 \text{ nm}^2$.

Two pairs of electromagnets generate a magnetic field either perpendicular or parallel to the film surface so that both polar and longitudinal hysteresis loops can be obtained without moving the sample. An inserted quarter waveplate makes the measured Kerr intensity proportional to the Kerr ellipticity.^[10]

As is well known, the clean Pt(001) surface is reconstructed exhibiting an (almost) incommensurate quasihexagonal overlayer residing on quadratic substrate below leading to a superstructure simply described as Pt(001)-hex.^[7–9] The sharp LEED pattern together with the clear STM image in our experiment

* Supported by the National Natural Science Foundation of China and the Ministry of Science and Technology of China (G001CB3095 and 2002CB613502).

** Email: kehe@aphy.iphy.ac.cn

©2005 Chinese Physical Society and IOP Publishing Ltd

[Figs. 1(a) and 1(b)] show that we have achieved a clean reconstructed surface. Figures 2(a)–2(d) show snapshots of the surface morphology after deposition of increasing amounts of Fe at room temperature. In earlier work^[11–14] it was observed that Au atoms could segregate to the very film surface upon Fe deposition, even up to considerable Fe coverage. Because of great similarities with the Fe/Au(001) system, Fe deposited on Pt(001) surface has almost the same char-

acteristics as Fe on Au(001). In the sub-ML range [Fig. 2(a)], the Pt atoms exchanged to the surface form new islands, which also exhibit the “hex” reconstruction. Then a dramatic decrease of long-range order takes place around 1.7 ML, at which there are notably no clear (1×1) LEED spots [Fig. 2(f)]. With further increasing thickness, *bcc*-Fe films develop with a clear (1×1) LEED pattern.

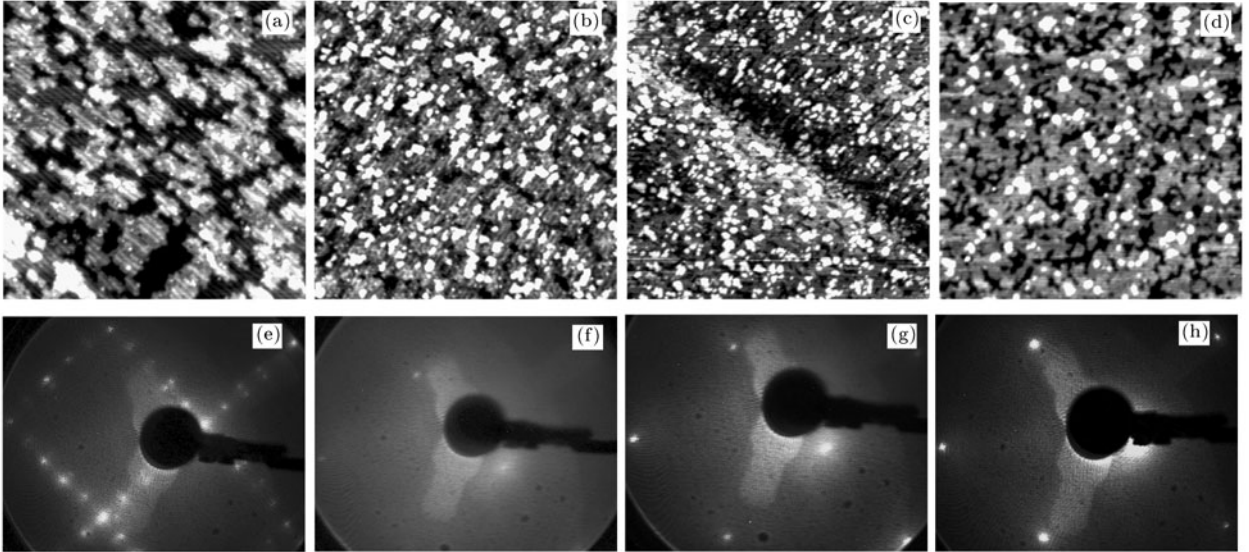


Fig. 2. STM images ($100 \times 100 \text{ nm}^2$) and LEED patterns of the as-grown Fe films on Pt(001) surface at different coverages: (a) and (e) 0.6 ML, (b) and (f) 1.2 ML, (c) and (g) 2.2 ML, (d) and (h) 3.3 ML.

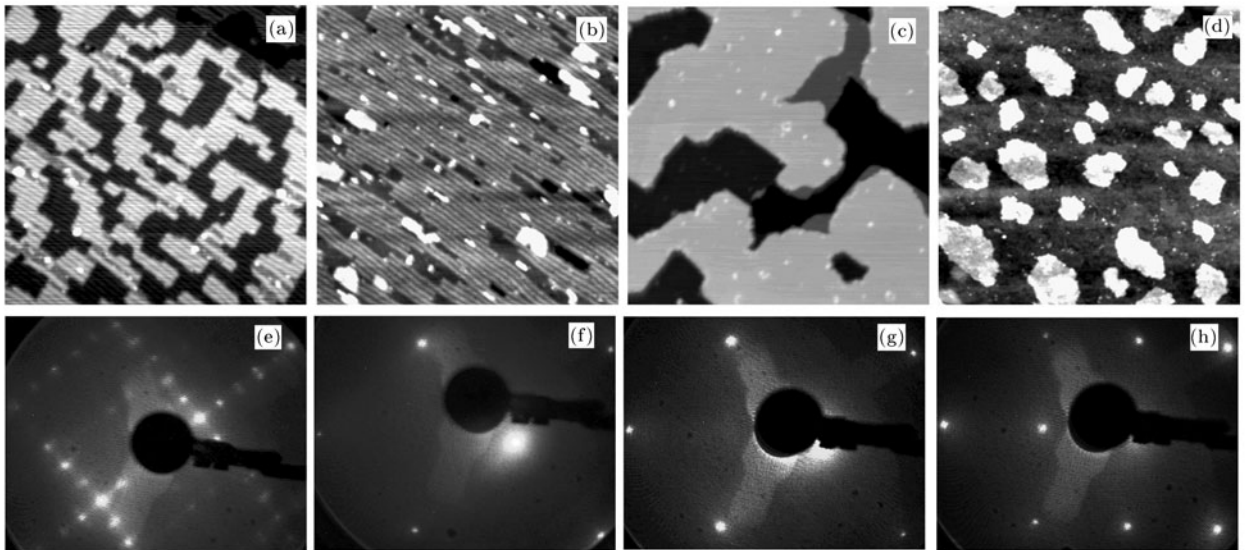


Fig. 3. STM images ($100 \times 100 \text{ nm}^2$) and LEED patterns of Fe films on Pt(001) surface for various coverages after annealing at $\sim 600 \text{ K}$: (a) and (e) 0.6 ML, (b) and (f) 1.2 ML, (c) and (g) 2.2 ML, (d) and (h) 3.3 ML.

After annealing, the contrast of the LEED spots with the background improves slightly. The LEED pattern develops to a sharp (1×1) pattern around 1.7 ML [Fig. 3(f)]. Surprisingly, $(\sqrt{2} \times \sqrt{2})$ LEED spots appear at $\sim 3.3 \text{ ML}$ thickness [Fig. 3(h)]. Fur-

ther STM images reveal that the Fe films become much smoother. We can easily say that when the sample is annealed at 600 K, Pt and Fe intermix with each other much more deeply^[6,15] and it is very possible that the $(\sqrt{2} \times \sqrt{2})$ reconstruction is due to ordered

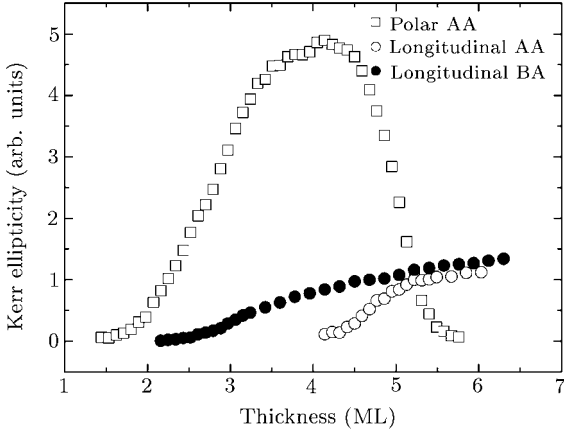


Fig. 4. Plot of remanence as a function of the thickness of the Fe film before and after annealing (BA and AA).

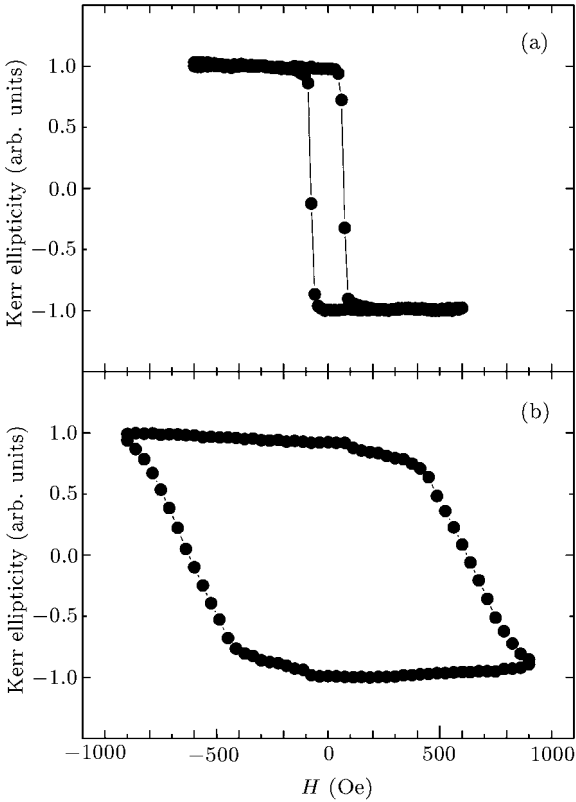


Fig. 5. Polar Kerr hysteresis loops of selected Fe thicknesses after annealing: (a) 4.0 ML, (b) 2.6 ML.

Pt–Fe alloy formation. Unfortunately we did not obtain any atomic resolution results indicating the Pt–Fe alloy structure by STM.

The *in situ* SMOKE measurement results are summarized in Fig. 4, where remanence is plotted as a function of the thickness of the Fe film. Initially the as-grown Fe film shows the in-plane easy axis in the thickness range studied (~ 7 ML), as is also the case for Fe/Pd(001),^[16] but quite different from Co/Pt(111) film^[17] which displays perpendicular magnetic anisotropy at low coverage. The magnetic remanence appears at ~ 2.2 ML Fe thickness, increases

quickly in the range 2–3.5 ML, and increases linearly above 3.5 ML thickness as clearly seen in Fig. 4. The absence of the Kerr signal below 2.2 ML thickness shows that the Curie temperature of Fe film below 2.2 ML is less than room temperature. The linear increase of the Kerr signal with film thickness above 3.5 ML simply reflects the additivity law for ultrathin ferromagnetic film.^[10]

After annealing, the magnetic properties of the film changes dramatically. The easy axis of magnetization switches from in-plane to perpendicular at low coverage. As the film thickness increases above 4.2 ML, the polar Kerr signal starts to decrease gradually and the longitudinal signal becomes observable. To our knowledge, this implies that an SRT occurs when the shape anisotropy, caused by dipolar interaction, overcomes the surface anisotropy. It is well known that the magnetic properties of ultrathin Fe films on Pd(001) show an intriguing dependence on the growth temperature.^[16] The room-temperature grown films show the in-plane easy axis for all coverages, while low-temperature grown films below 2.5 ML exhibit the perpendicular magnetic anisotropy (PMA). The formation of disordered Fe–Pd alloy near the interface is suspected to determine the observed dependence of Fe film magnetic behaviour on the growth temperature. It is noteworthy that Co/Au^[18] and Co/Pd^[19] multilayers also exhibit in-plane magnetic anisotropy induced by interfacial alloying and interfacial roughness. This implies that interface roughness and interdiffusion might tend to decrease the strength of the PMA.^[20] However our results suggest that after annealing at 600 K, for coverages below 4.2 ML the in-plane signal disappears and the PMA of the film is enhanced. In a recent SMOKE experiment on Co/Pt(111), Shern *et al.* also found that the perpendicular Kerr signal doubles in intensity for 1 ML Co overlayer after annealing at 710 K.^[17] The formation of an ordered Co–Pt alloy has been suggested by Train *et al.* to explain the PMA enhancement.^[21] Our results may similarly be explained by ordered Fe–Pt alloy formation. A close look at the magnetic properties of 3–4 ML Fe films reveals that there is a dramatic change in the coercivity of the hysteresis loop at ~ 3.3 ML (Fig. 5), the thickness at which the $(\sqrt{2} \times \sqrt{2})$ LEED pattern appears. We can say that there are two magnetic phases (hard and soft) in this transition. It is well known that FePt is a magnetically hard phase while Fe₃Pt is a magnetically soft phase.^[22] The L₁₀ FePt phase has a chemically ordered *fcc* structure with $a = 0.3861$ nm and $c = 0.3788$ nm; Fe₃Pt phase has an ordered L₁₂ structure with $a = 0.3730$ nm. Their (001) surfaces have precisely a $\sqrt{2} \times \sqrt{2}$ relation.^[23] Thus we can easily understand that while Fe thickness remains below 3.3 ML, the ordered FePt (L₁₀) alloy with large coercivity forms stably; and as the Fe thickness increases,

less Pt diffuses into the Fe film and an ordered Fe₃Pt (L1₂) alloy with smaller coercivity appears to produce a $\sqrt{2} \times \sqrt{2}$ LEED pattern. The easy magnetic axis of bulk FePt ordered alloy is along the [001] direction,^[24] i.e. perpendicular to the film in our case, while the easy axis of Fe film is in-plane. The competition between them contributes to the SRT we observed.

In summary, we have examined the structural and magnetic properties of ultrathin Fe films grown on clean Pt(001) substrate. For as-grown film only in-plane magnetic anisotropy is observed. After annealing at elevated temperature, the Fe film develops a perpendicular magnetic anisotropy at low coverage and then is transverse to in-plane anisotropy as Fe film thickness increases. Structural investigation reveals that the as-grown Fe film on Pt(001) has the same structure as Fe on Au(001). After annealing Fe/Pt intermix with each other deeply and the ordered FePt (L1₀) and Fe₃Pt (L1₂) alloys form, which is responsible for the significant changes in the magnetic properties of the Fe film on Pt(001).

References

- [1] Falicov L M, Pierce D T, Bader S D, Gronsky R, Hathaway K B, Hopster H J, Lambeth D N, Parkin S S P, Prinz G, Salomon M, Schuller I K and Vitoria R H 1990 *J. Mater. Res.* **5** 1299
- [2] Himpsel F J, Ortega J E, Mankey G J and Willis R F 1998 *Adv. Phys.* **47** 511
- [3] Wang X Y, Zhang Y P, Li Z Y, Shen D F and Gan F X 2003 *Chin. Phys. Lett.* **20** 1359
- [4] Sakurai M 1994 *J. Appl. Phys.* **76** 7272
- [5] Visokay M, Lairson B M, Clemens B M and Sinclair R 1993 *J. Magn. Magn. Mater.* **126** 136
- [6] Hufnagel T C, Kautzky M C, Daniels B J and Clemens B M 1999 *J. Appl. Phys.* **85** 2609
- [7] Behm R J, Hösler W, Ritter E and Binnig G 1986 *Phys. Rev. Lett.* **56** 228
- [8] Van Hove M A, Koestner R J, Stair P C, Biberian J P, Kesmodel L L, Bartos I and Somorjai G A 1981 *Surf. Sci.* **103** 189
- [9] Heilmann P, Heinz K and Müller K 1979 *Surf. Sci.* **83** 487
- [10] Qiu Z Q and Bader S D 1999 *J. Magn. Magn. Mater.* **200** 664
- [11] Himpsel F J 1991 *Phys. Rev. B* **44** 5966
- [12] De Rossi S, Ciccacci F, and Crampin S 1995 *Phys. Rev. B* **52** 3063
- [13] Opitz R, Löbus S, Thissen A, and Courths R 1997 *Surf. Sci.* **370** 293
- [14] Blum V, Rath Ch, Müller S, Hammer L, Heinz K, Carcía J M, Ortega J E, Prieto J E, Hernán O S, Gallego J M, Vázquez de Parga A L, and Miranda R 1999 *Phys. Rev. B* **59** 15966
- [15] Lee S K, Kim J S, Kim B, Cha Y, Han W K, Min H G, Seo Jikeun and Hong S C 2001 *Phys. Rev. B* **65** 014423
- [16] Liu C and Bader S D 1990 *J. Appl. Phys.* **67** 5758
Liu C and Bader S D 1991 *J. Magn. Magn. Mater.* **99** L25
Liu C and Bader S D 1991 *J. Vac. Sci. Technol. A* **9** 1924
- [17] Shern C S, Tsay J S, Her H Y, Wu Y E and Chen R H 1999 *Surf. Sci.* **429** L497
- [18] Den Broeder F J A, Kuiper D, Van de Mosselaer A P and Hoving W 1988 *Phys. Rev. Lett.* **60** 2769
- [19] Reim W and Wachter P 1985 *Phys. Rev. Lett.* **55** 871
- [20] Kim J, Lee J W, Jeong L R, Shin S C, Ha Y H, Park Y and Moon D W 2002 *Phys. Rev. B* **65** 104428
- [21] Train C, Beauvillain P, Mathet V, Penissard G and Veillet P 1999 *J. Appl. Phys.* **86** 3165
- [22] Zeng H, Li J, Liu J P, Wang Z L and Sun S 2002 *Nature* **420** 395
- [23] Li J, Wang Z L, Zeng H, Sun S and Liu J P 2003 *Appl. Phys. Lett.* **82** 3743
- [24] Lairson M, Visokay M R, Sinclair R and Clemens B M 1993 *Appl. Phys. Lett.* **62** 639